IEEE Access
Multidisciplinary | Rapid Review | Open Access Journal

IEEE POWER & ENERGY SOCIETY SECTION

Received 6 March 2024, accepted 10 April 2024, date of publication 19 April 2024, date of current version 20 May 2024.

Digital Object Identifier 10.1109/ACCESS.2024.3391298

RESEARCH ARTICLE

Maximum Reserved Capacity of Aggregated Electric Water Heaters Virtual Battery for Peak Management

ISMAIL ARAFAT, (Graduate Student Member, IEEE), HOSSEIN SHOKOUHINEJAD, EDUARDO CASTILLO GUERRA, (Senior Member, IEEE), JULIAN MENG, (Senior Member, IEEE), AND JULIAN L. CARDENAS-BARRERA, (Member, IEEE)

Department of Electrical and Computer Engineering, University of New Brunswick, Fredericton, NB E3B 5A3, Canada

Corresponding author: Ismail Arafat (i.arafat@unb.ca)

This work was supported by the National Research Council of Canada and Saint John Energy.

ABSTRACT This paper introduces new insights into the integration of thermostatically controlled loads (TCLs) as hybrid energy sources for grid ancillary and demand response services. Leveraging a generalized virtual battery (VB) model emerges as an effective approach to determine maximum reserve capacity of these aggregated devices. Our research extends the VB model and endeavors to establish a pragmatic framework for EWH control for peak shaving and managing the payback effect. The importance of aggregator capacity in mitigating the impacts of TCL external control, such as customer comfort and safety, is emphasized. Electric water heaters (EWHs) are used as the residential TCL device given their extensive availability and thermal capacity. Two TCL control scenarios, OFF control and ON/OFF control are compared using the Model Predictive Control (MPC) method. The ON/OFF control was found to improve peak shaving capability by approximately 47% when compared to the more rudimentary OFF control mechanism. The main contributions of this study are threefold: assessment of maximum reserve capacity using a modified VB model, creation of a reference control signal based on this result, and development of effective control strategies for managing the payback effect when maximal reserves are utilized. The robustness of the maximum capacity estimation is analyzed through a sensitivity analysis mainly driven by variations in hot water consumption and communication loss. Comprehensive and comparative simulation results show improved capabilities in the utilization of the maximum reserved energy of loads, minimizing the expected payback to avoid additional energy peaks and assessing the impacts of external factors that can affect the expected maximum capacity of the VB.

INDEX TERMS Demand response, peak management, model predictive control, thermostatically controlled loads, virtual battery.

NOMENCLATURE

N	Number of TCLs.
$\theta^k(t)$	Temperature of the water in the k^{th} EWH at time instant t.
$\theta^k_{out}(t)$	Ambient air temperature outside the k^{th} EWH at time instant t.
$\theta^k_{in}(t)$	Incoming water temperature of the k^{th} EWH at time instant t.
R^k	Thermal resistance of the k^{th} EWH.
C^k	Thermal capacitance of the k^{th} EWH.
ρ	Density.
c_p	Specific heat.
$\omega^k(t)$	Demand of the k^{th} EWH at time instant t.
P^k_{rate}	Rated power of element.
$m^k(t)$	State of the k^{th} EWH at time instant t, $m^k(t) \in \{1, 0\}$.

The associate editor coordinating the review of this manuscript and approving it for publication was Ravindra Singh.

© 2024 The Authors. This work is licensed under a Creative Commons Attribution-NonCommercial-NoDerivatives 4.0 License.
For more information, see https://creativecommons.org/licenses/by-nc-nd/4.0/

θ^k_{set}	Setpoint temperature of the k^{th} EWH.
δ^k	Mid-Hysteresis band width of the k^{th} EWH.
Δt	Small-time increment, $\Delta t \ll 1$.
P_{base}	Baseline Power.
P_{agg}	Aggregator Power.
$X_{agg}(t)$	State of charge of the virtual battery at time instant t.
$U(t)$	Power charge/draw of the virtual battery at time instant t.
X_{min}, X_{max}	lower/upper energy capacity limits of the virtual battery.
$P_{min}(t)$, $P_{max}(t)$	Discharge/charge power limits at time instant t.
α, β	Parameters.
Φ	Virtual battery model.
$X_{ref}(t)$	Desired charging/discharging level (Energy reference signal) at time instant t.
$\varepsilon_x(t)$	Energy error signal at time instant t.
$P_{ref}(t)$	Power reference signal at time instant t.
$\varepsilon_p(t)$	Power error signal at time instant t.
N_x, N_p	Prediction horizons.
PP_p	Shaving capacity to payback index.

I. INTRODUCTION

A. GENERAL

Peak power demands (referred to as ''peak periods'' in this paper) can threaten electrical grid stability in a daily manner. Typically, this occurs twice a day (morning and evening) in the winter season when demand is more critical. Utilities generally use more costly spinning reserves to meet peak demands to ensure grid stability and customer comfort. This can increase the customer electricity price [1], contribute to harmful effects on the environment and result in poor generation efficiency [2]. A solution to reduce these costs is to control electric thermal loads through programs such as Demand Response (DR). DR holds particular significance for utilities as it offers avenues for cost reduction, enhancement of grid stability, and effective peak management without substantial investments in additional capacity infrastructure [3], [4]. The effective management of an TCLs aggregation often requires a central higher-level control system denoted as a virtual power plant (VPP) [5]. The VPP integrates the TCLs and other resources into energy markets, while also providing essential grid services [5], [6].

B. OVERVIEW OF THE DR IN RESIDENTIAL LOADS

DR controls a group of loads (i.e., aggregators [7]) such as EWHs, heat pumps (HP), Air Conditioning (AC), base boards (BB), electric vehicle (EV), and electric thermal storage (ETS) systems. TCLs are commonly encountered in the residential sector consumption, and for instance, about 20% of the energy produced in the United States [8], [9], [10] is utilized for such loads. The number of TCLs are also expected to increase due to greater demands for heating, cooling, and population growth. The opportunity exists for such devices to contribute significant capacity for ancillary services such as peak shaving [1], [2], [11], [12], [13], [14]. Their maximum capacity can be used as an emergency backup resource, deployable at the utility level for peak shaving and frequency restoration purposes. Substantial reductions in energy costs can be achieved through optimal management strategies. Moreover, such management practices have the potential to incentivize customer participation in Local Energy Market (LEM) schemes and peer-to-peer (P2P) trading, offering tangible rewards and benefits. EWHs are particularly appealing due to their ubiquity and aggregated thermal energy capacity. In Canada, EWHs account for 19.3% of the average energy used in the residential sector and 5.7% of the average energy used in the commercial sector, thus accounting for 17% of the total energy consumption [10], [15], [16]. According to [15], this is the second highest energy consumption load in Canada.

A significant number of research papers and pilot projects support the use of EWHs as a good candidate for demand-side management applications [17], [18], [19], [20], [21], [22], [23], [24], [25]. EWHs exhibit commendable thermal proficiency and possess favorable thermal inertia, facilitating the efficient storage of energy in the form of heat within a relatively abbreviated timeframe. Moreover, these systems can be briefly deactivated without detrimentally impacting the comfort of end-users [18]. This attribute ensures a certain energy capacity depending on the thermal state of the EWH. The study conducted in [17] summarizes experimental solutions to reduce load demand of EWHs by motivating customers to reduce energy consumption during predefined peak periods based on pilot studies. The study reported a peak reduction of 4.2% in Norway by utilizing 50% of EWHs enrolled in a DR program. The investigation in [10] examined a cohort of 20,000 EWHs participating in a DR program. The findings substantiated that the morning peak demand could be reduced by an average of 24%, with exceptional cases achieving up to 31.3% reduction during the evening peak period. The issue of uncertainty arising from the water consumption patterns of EWH users is discussed in [16] and [19]. The simulation outcomes indicate no discernible adverse effects on customer comfort when implementing a reduction of 500Wh per EWH per day. It is worth emphasizing that the study could be enhanced by conducting an in-depth analysis of the optimal utilization of the maximum capacity of EWHs. The study conducted in [20] provides an economic analysis and compares the use of various TCLs and batteries for peak shaving. The study achieved a 20% peak reduction without determining the maximum limit of energy storage. A scalable controller for better management of EWHs is proposed in [21]. It provides 8.8% additional cost saving and better peak shaving. A tool for quantifying the reserve capacity of EWH and other TCLs is applied in [19] by calculating availability curves of EWH. Although the EWH aggregation literature is extensive, to this author's knowledge, the maximum theoretical reserved capacity for

this type of aggregator has not been fully addressed. This is a key contribution of this paper and will allow utilities to assess the full dispatch capabilities provided by TCLs. A comparative analysis of the existing literature is provided in Table 1.

Another major focus of our paper is limiting the payback effect after a peak-shaving event. This is characterized by TCLs attempting to compensate for the previous OFF period, thereby generating a new peak in energy demand. Previous research has provided a limited analysis of this phenomenon and how to best mitigate negative impacts. Authors in [22] provide a Norwegian study on how to use EWHs as a reserved capacity for frequency restoration and peak demand curtailment without estimating or utilizing the maximum aggregator capacity. Their results show a potential power reserve of 53.9% at morning peak times that can last for up to 61 minutes. The study also found that about 60% of TCLs can contribute to the payback for various peak shaving scenarios.

Large scale-aggregation of EWHs can be controlled to reduce consumption in the megawatt scale. The authors of [23] consider 10,000 EWH units, and their approach can shave up to 5 MWh and dispatch 30–43 MW at any given time. However, a system of this size will most likely experience a significant payback effect for multiple hours before restoring normal aggregator behavior. These studies provide several formulas to measure the payback effects but do not provide any methods to limit secondary load peaks due to this phenomenon. The researchers in [24] and [25] have devised a system aimed at tracking power references within a packetized energy management system. The functionality of this system encompasses communication traffic and the direct integration of TCLs with the VPP level.

The utilization of VB model serves multiple purposes within the energy management landscape, it is employed to aggregate capacity [8], and to facilitate frequency regulation [26], while also serving as the foundation for management and planning tools [18], [27]. In comparison, the integration of battery storage systems (BSS) at both residential and community scales contributes to enhanced control flexibility and cost savings [28], [29], [30]. Recent research has focused on exploring the integration of BSS with LEM and P2P systems, as in [28], [29], [30], [31], and [32]. Battery systems, virtual or otherwise, represent a promising avenue in energy management and trading in LEMs. This is mainly based on the availability of prosumers (consumers capable of generating energy through photovoltaic panels, wind turbines, and BSS). Unlike BSS, which primarily comprises of dedicated battery units, the VB represents a broader spectrum of household residential devices with energy storage capabilities that are controllable. As expected, there are significant challenges concerning the integration of TCLs and their associated VB capacity within LEM frameworks, as well as optimizing capacity trading to benefit customers, utilities, and grid stability. However, the utilization of household TCL devices for energy storage would serve as a valuable resource for supplying the fundamental grid ancillary services with marginal infrastructure costs. Moreover, it would increase the energy capacity available for trading from the prosumers, while promoting and expanding demand response programs with accessibility to various distributed energy resources. It is envisioned that customer participation will be incentivized through rewards aimed at facilitating access by the VB to their devices, thereby encouraging greater participation in the program.

C. OBJECTIVES AND CONTRIBUTIONS

The primary objective of this paper is extend the original VB model presented in [8], [18],and [26] to determine the maximum reserve capacity of an EWH aggregator. As expected, the maximum reserved capacity serves as a critical determinant of the aggregator's capability for peak shaving. Also, the payback effect is anticipated to be more pronounced due to our focus on maximum capacity shaving during peak periods. Our VB model will offer insight into the repercussions of peak shaving and facilitate an algorithmic approach to effectively manage any adverse effects. The contributions of the research are:

1) Ensure the maximum utilization of aggregator capacity during peak shaving operations through the incorporation of the VB model as an interface within the higher-level control scheme where the energy bid is ordered.
2) Administer and regulate the TCLs aggregator to mitigate the repercussions of payback linked to the peak shaving process.
3) Development of a utility level framework showing the maximum reserved capacity, anticipated payback, durations of shaving and payback, charging/discharging times and rates, and other relevant parameters.

This paper is organized as follows. The background information of EWH and VB models is given in Section II. The control strategies are presented in Section III. A numerical example to demonstrate the validity of the proposed approach is analyzed in Section IV, followed by the conclusion remarks in Section V.

II. BACKGROUND

For our research, we assume the utilization of a homogenous EWH aggregator with a predefined water consumption profile that is scaled to a city with 70,000 habitants in Canada. The hot water consumption profiles are generated based on statistical studies and assumed to follow different water consumption profiles (i.e., morning, evening, and sparse users) [33], [34]. Two modes of EWH control are considered for the utilization of the maximum reserved capacity. The first mode is achieved by generating only OFF signals where the ON signal is controlled by the internal thermostat of the EWH. The second mode generates both ON/OFF control signals in addition to internal thermostatic control which can be overridden. The VB model is utilized to define the

TABLE 1. Summary of related works in peak shaving and proposed work.

	Maximum capacity	Payback Control	Sensitivity		Customer satisfaction
			water usage	communication	
[2], [11], [12]	X	X	-	X	✓
[10], [13], [14], [17], [20]	X	X	X	X	✓
[16], [19], [21]	X	X	✓	X	✓
[22], [23]	X	✓	X	X	✓
Proposed	✓	✓	✓	✓	✓

aggregator performance in terms of peak shaving capacity and the optimal deployment of TCLs.

A. EWH HYBRID MODEL

The differential equation model of the thermal characteristics of each EWH (indexed by k) with a single heating element is described as follows:

$$\dot{\theta}^k(t) = \frac{1}{R^k C^k}\left(\left(\theta^k_{out}(t) - \theta^k(t)\right) + \rho c_p R^k \omega^k(t)\left(\theta^k_{in}(t) - \theta^k(t)\right) + R^k m^k(t) P^k_{rate}\right) \tag{1}$$

This hybrid model is widely used in the literature [8], [10] where the temperature of the water is assumed to be uniform across the tank. Each EWH has a temperature setpoint θ^k_{set} with a hysteretic ON/OFF local thermostat control so that the operating state of $m^k(t)$ is given by:

$$m^k(t) = \begin{cases} 1 & \theta^k(t) < \theta^k_{set} - \delta^k \\ 0 & \theta^k(t) > \theta^k_{set} + \delta^k \\ m^k(t-\Delta t) & otherwise \end{cases} \tag{2}$$

All the above parameters are known, except for the hot water demand. This study uses past household data to develop a water usage model for accurate prediction of individual EWH temperature profiles [33].

It is important to note that when the EWH is operated by its own thermostat control, the water heater element turns ON in two circumstances: 1) the water temperature has dropped below the minimum setpoint primarily due to conduction heat losses; and 2) a large amount of hot water has been drawn and replaced with colder incoming water. If the water temperature associated with either case drops by $\theta^k_{set} - \delta^k$, the element will be ON to re-heat the water to the set temperature. In the first case, the ON duration is predictable and relatively consistent. The second case is more complex where the heating element is turned ON for a variable time duration depending on the amount of hot water drawn and inlet water temperature. For the latter case, water consumption profiles are necessary to estimate the energy storage capacity of the EWHs.

B. BASELINE POWER

Consider a continuous thermal model as an approximation to the simple model in (1) where each EWH has a continuous power input $P^k(t) \in \{0, P^k_{rate}\}$. Therefore, the continuous thermal model in ON state (i.e., $m^k(t) = 1$) can be written as [8], [10]

$$\dot{\theta}^k(t) = \frac{1}{R^k C^k}\left(R^k P^k(t) + \left(\theta^k_{out}(t) - \theta^k(t)\right) + \rho c_p R^k \omega^k(t)\left(\theta^k_{in}(t) - \theta^k(t)\right)\right) \tag{3}$$

where the EWH temperature increases with the rate of $R^k P^k(t)$. The second term in (3) is the temperature decay associated with the conduction heat loss and the third term is related to the heat loss because of the hot water demand. These heat losses are used to derive the baseline power required to keep the temperature at the desired setpoint. Equation (4) shows the power necessary to offset heat loss:

$$P^k_n(t) = \frac{1}{R^k}\left(\theta^k_{set}(t) - \theta^k_{out}(t)\right) + \rho c_p \omega^k(t)\left(\theta^k_{set} - \theta^k_{in}(t)\right) \tag{4}$$

Consequently, the baseline power of a population of N EWHs with the hybrid model can be approximated by the aggregate baseline power with the continuous model as follows:

$$P_{base}(t) = \sum_{k=1}^{N} P^k_n(t) \tag{5}$$

Additionally, the aggregated power consumption of a collection of EWHs at time t is given by:

$$P_{agg}(t) = \sum_{k=1}^{N} m^k(t) P^k_{rate} \tag{6}$$

C. VIRTUAL BATTERY MODEL

The energy stored in each EWH is directly proportional to the temperature difference between the current temperature and the set point temperature. The EWH hysteresis bandwidth between thermostat ON and OFF temperatures can be accumulated to provide some insight to the aggregator capacity. Using this idea, the VB model involves defining the State of Charge (SOC) of the EWH aggregator, representing the combined energy of the aggregator encompassing both baseline

and reserved energy. The formulation for the aggregator SOC, $X_{agg}(t)$, is given by [8], [26], [35], [36]:

$$X_{agg}(t) = \sum_{k=1}^{N} C^k \left(\theta^k(t) - \theta^k_{set}\right) \tag{7}$$

The thermal constraint of EWH temperature as follows:

$$\theta^k_{set} - \delta^k \leq \theta^k(t) \leq \theta^k_{set} + \delta^k \tag{8}$$

The VB serves as a concise abstract representation accommodating both homogenous and heterogeneous aggregators (i.e., various TCL types) [8]. The VB model is a valuable tool for investigating the potential capacity inherent in fleet of TCLs [18], [35], [37]. The first-order linear VB model is defined as:

$$\dot{X}_{agg}(t) = \alpha X_{agg}(t) + \beta U(t) \tag{9}$$

$$X_{min} \leq X_{agg}(t) \leq X_{max} \tag{10}$$

$$P_{min}(t) \leq U(t) \leq P_{max}(t) \tag{11}$$

$$\mathrm{U}(t) = P_{agg}(t) - P_{base}(t) \tag{12}$$

The parameters α and β are determined through the application of system identification methods. Specifically, the System Identification Subspace Method as detailed in [38] is implemented in conjunction with the model to ascertain these parameters. These parameters undergo adjustments in accordance with the quantity and type of aggregated devices. The VB model given in (9)- (12) is used to aggregate the reserved capacity of each category of residential loads. It is independent from complicated thermal dynamics represented by equations (1)-(4). The constraints governing the VB capacity limits are regulated by the δ^k in (8). The input power $U(t)$ of the VB is limited as illustrated in (11). The minimum allowable power $P_{min}(t)$ that can be charged or discharged from the VB is constrained by the baseline power (13). Conversely, the maximum power $P_{max}(t)$ that can be supplied to or drawn from the VB depends on the power of EWHs that not part of the baseline power (14), the VB parameters are as follows [8], [18], [26]:

$$P_{min}(t) = -P_{base}(t) \tag{13}$$

$$P_{max}(t) = \sum_{k=1}^{N} P^k_{rate} - P_{base}(t) \tag{14}$$

$$X_{max} = \sum_{k=1}^{N} C^k \delta^k \tag{15}$$

$$X_{min} = -\sum_{k=1}^{N} C^k \delta^k \tag{16}$$

Therefore, the VB model (Φ) defined in (7)-(12) is specified by the parameters in (13)-(16), and can be written as follows:

$$\Phi := (X(t), \alpha, \beta, P_{min}(t), P_{max}(t), X_{min}, X_{max}) \tag{17}$$

This model is an extension of the basic VB model and can monitor the EWH aggregator energy level, as well as providing information about customer comfort. The aggregated energy capacity of EWHs is the sum of the individual TCLs ability to store energy between charge and discharge time. The individual characteristics of each EWH, such as set point, hysteresis band, size, energy demand, and daily consumption profile, present a significant challenge for accurately modeling the aggregator reserved energy. The limits of the VB model are directly impacted by the unique characteristics of each EWH, which must be accounted for in the development of a dynamic algorithm that adjusts the aggregated limits. For example, the group of EWHs that discharge beyond the lower limit of hysteresis band cannot be turned OFF and are unavailable for control. Consequently, the power limit is continuously updated based on the current state of the EWHs. The water temperature of a tank is another key factor in determining the energy capacity of the EWH. The aggregated state of charge (SOC) is the stored energy available at each time step given by (7) and is an indicator of the VB charge status. If the aggregated SOC reaches the lower or upper VB limit, all EWHs are at the boundary of the hysteresis band temperature at the same time. These two limits exhibit a notably low probability of occurrence, particularly in scenarios where the number of EWHs is substantial. These inferences are drawn from an analysis of the daily power profiles of the EWHs, the corresponding random daily hot water consumption, and gathered SOC results without affecting the user's comfort. The aforementioned factors result in a time-varying estimation of the aggregator maximum capacity. In summary, full of the VB capacity in practice cannot be achieved and utilizing the maximum available capacity in peak shaving is another challenge.

III. PROPOSED STRATEGY

This investigation assumes a peak shaving management scheme that has three hierarchical levels: a load level (low level), an aggregator level (intermediate level), and a virtual power plant (VPP) level (high level). The present study examines a potential trading agreement between the VPP and VB aggregator, wherein the VPP submits its request for peak management with an adequate lead time. This contract encompasses provisions to allow the VB to lower the available capacity for inadequate lead times and in the event of a communication loss with EWHs.

The agreement permits the VB to reject the commitment if no capacity is available. The energy transaction between these three levels is shown in Fig. 1 and conceived as follows. First, each EWH at the load level sends its data (i.e., current temperature, power rating, setting point, etc.) to the aggregator level. The activation of the aggregator level is contingent upon receiving commands from the VPP, and undertaking the following tasks: 1) construct the VB model for the connected loads based on the received information, 2) estimate the maximum of stored capacity that the aggregator can commit to peak shaving based on the mathematical model and hot

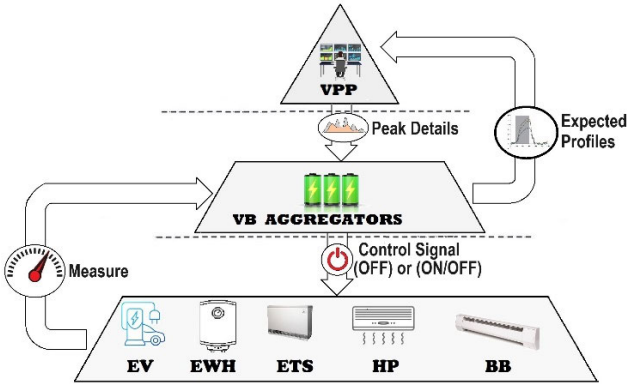

FIGURE 1. Data flow between the hierarchical levels.

water consumption profile, as given in equations (7)(15)(16), and 3) share the information with the VPP level. The VPP monitors the energy market dynamics, the forecasted load consumption, and the available generation resources throughout the day. The goal is to maximize load shaving using TCLs during peak periods as this can yield substantial energy cost reductions. The VPP also requires relevant information (i.e., shaving percentage, discharge SOC, expected payback period…etc.) for maintaining a smooth transition post-peak period. The VPP plays a pivotal role in allocating target power profiles to the aggregator based on its stored energy and the desired contribution level. Consequently, the aggregator attempts to align itself with the dispatched power profile received from the VPP. This requires direct control over EWHs to adhere to the reference power signal sent by the VPP.

A. PEAK PERIOD

The implemented management framework distinguishes between two interrelated peak periods occurring at distinct control levels. The initial period pertains to the utility level, denoted as the VPP level peak, and initiates when the power demand surpasses a predefined threshold as determined by the VPP. Concurrently, the second period is specific to the local aggregator, commencing during the timeframe of highest demand, surpassing the average aggregator demand. This study aims to strategically utilize the aggregator's local peak period to shave the VPP peak. The VPP level peak aggregates demand from various loads, including EWHs, Heating, Ventilation, and Air Conditioning systems (HVACs) and others. In practice, the utility peak period occurs when the cumulative load requires the activation of reserve energy resources. From a technical perspective, the EWHs aggregator local peak interval should ideally align within the duration of the VPP level peak. However, occasional variations may occur, particularly in the presence of substantial load types other than EWHs. The optimal benefit for the management system is realized when the aggregator's peak period aligns with the VPP peak period, ensuring maximum capacity from the aggregator during this crucial interval.

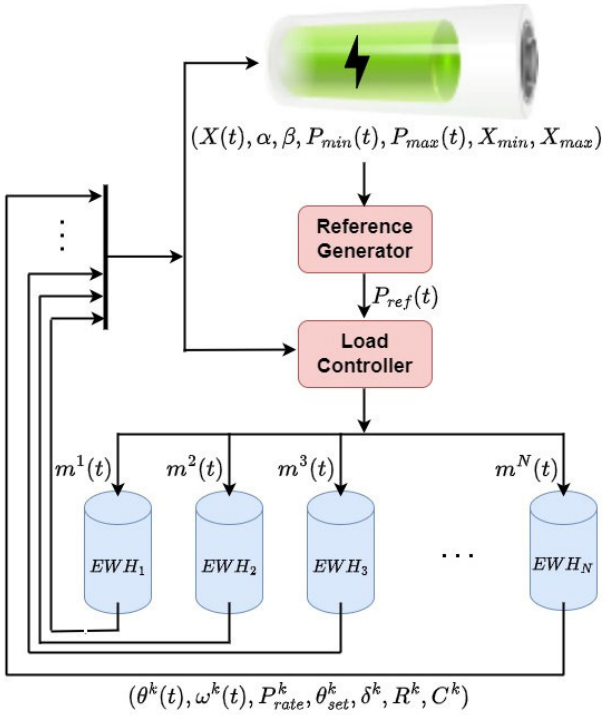

FIGURE 2. Schematic of proposed aggregator.

B. AGGREGATOR CONTROL

The simulations in this study consist of both off-peak periods where peak shaving is not requested and the peak period where shaving is requested. The control system assumes two controllers, the first is the thermostat control representing the EWH internal control. Thermostatic control is the default for periods as given in (2) when no shaving services are required. The second controller (i.e., OFF or ON/OFF) is activated according to the desired reference signal and respecting the individual management scheme discussed in (2),(8). This paper proposes an aggregator level strategy to estimate the maximum capacity that the aggregated EWHs can provide to the VPP level during peak shaving functions. The schematic diagram of the proposed aggregator control strategy shown in Fig. 2 includes a MPC reference controller and a time varying MPC load controller. The MPC reference controller generates power reference signal based on the VB model. The reference profile respects the VB constraints and the aggregator power limits and is fed to the load controller unit. The MPC load controller acts as a central control unit. It is designed to create control signals (regulation signals, $m^k(t)$) such that the aggregated power tracks the power reference signal of maximum capacity. As stated earlier, this study considers two scenarios in generating EWHs control signal.

1) OFF CONTROL SCENARIO

The control signals can only override the ON state of EWH, and safety standards prevent the controller from overriding the OFF state of EWHs. The EWHs are turned ON only by

the internal thermostat (i.e., temperature decays to $\theta_{set}^{k} - \delta^{k}$. The controller's goal during the peak period is to reduce the energy consumption of the EWH by turning them OFF while satisfying the comfort of users. Consequently, the VB is depleted to a minimum (depending on the available capacity) with a specified discharge rate. The payback control period starts immediately after finishing the peak period. Normally, when the peak shaving controller is removed, a significant number of EWHs will turn ON to compensates the previous outage. The SOC of the VB would be at its minimum value and the VB should be charged gradually in the payback period. Hence, employing a controller during this period is crucial to prevent creating an uncontrolled peak and to manage the changing states of EWHs in a gradual manner.

2) ON/OFF CONTROL SCENARIO

The input controller in this scenario can override both ON and OFF states of EWH thermostat. It gives the controller more options as compared to the first scenario. Special attention is required when overriding the thermostat control signal, may affect user comfort and safe water temperature protocols. Moreover, in addition to the peak period and payback period, ON/OFF control can utilize a pre-charging period to 1) increase the number of EWHs available to be turned OFF during peak period and 2) considerably reduce the payback control duration and negative payback effects. Pre-charging is the period when the EWHs are switched ON gradually before the peak period starts as long as user comfort is maintained. The duration of this period depends on the aggregator capacity, SOC of the VB, and charging rate. The goal is to charge the VB at a specific rate to its maximum capacity prior to an anticipated peak event.

C. REFERENCE GENERATOR AND MPC FORMULATION

The VB model given by equations (9)-(12) establishes a relationship between SOC and instantaneous power. It gives an idea of the aggregator capacity to be allocated in every sample during peak shaving process. The VB capacity, $X_{agg}(t)$, is influenced by the input power and is limited by the hysteresis bandwidth and aggregation size. The input signal $U(t)$, represents the power drawn from the VB with the goal of using the SOC to track the desired charging/discharging level during all three control periods. The MPC was chosen due to its established efficacy in optimizing the performance of dynamic systems. Developed to address the intricacies of complex and nonlinear systems, MPC iteratively predicts future system behavior, informing control decisions based on these predictions. The formulation of MPC begins with constructing a mathematical model describing the system's dynamics and behavior, derived from physical laws, data-driven techniques, or a combination thereof. Subsequently, the MPC controller utilizes this model to forecast the system's response to diverse control inputs over a finite prediction horizon. The controller seeks to determine control inputs that minimize a cost function, representing objectives such as trajectory tracking or energy consumption reduction. This optimization problem is solved iteratively at each time step, yielding a sequence of control inputs. This iterative process enables MPC to dynamically adapt and respond to system changes and disturbances, rendering it a versatile and robust control strategy widely employed across diverse industries, including robotics, process control, and autonomous vehicles. The primary function of the MPC controller in our specific scenario is to adhere to and synchronize with the VPP requested capacity sent to the aggregator. The tracking error of the VB energy level can be defined as:

$$\varepsilon_x(t) = X_{ref}(t) - X_{agg}(t) \tag{18}$$

Initially, the energy reference signal is created to achieve VB charging gradually with a predetermined rate during pre-charging period. This period is useful to charge the VB to its maximum prior to peak shaving. The MPC controller's goal is to deplete the VB at a reasonable rate during peak shaving and ensure that the stored energy is available for the complete peak period. If the discharge rate is too high, the available EWHs will turn OFF at the beginning of the peak period and no capacity is left for the remaining of the peak period. It is reasonable to set the VB discharge rate so that the shaved energy is uniform during this period. Finally, the reference energy signal again guides the proper VB charging rate during the payback period. This charging rate should be designed such that the probability of a residual peak is low, or that the payback duration is not overly long. Therefore, charging and discharging VB rates in all three control periods is a challenging issue that should be investigated in more detail. Now, by defining the objective function as:

$$J_x(t) = \int_{t}^{t+N_x} \varepsilon_x^2(\tau)\, d\tau \tag{19}$$

The input signal $U(t)$ is achieved by solving the following optimization problem:

$$\min J_x(t)$$
$$\text{Subject to} \quad \begin{cases} \dot{X}_{agg}(t) = \alpha X_{agg}(t) + \beta U(t) \\ X_{min} \le X_{agg}(t) \le X_{max} \\ P_{min}(t) \le U(t) \le P_{max}(t) \end{cases} \tag{20}$$

Equation (20) indicates that the desired SOC will be achieved if the power drawn from the VB is equal to desired input signal $U(t)$. The new reference is dealing with power and labeled as demand power reference signal and is defined as follows:

$$P_{ref}(t) = U(t) + P_{base}(t) \tag{21}$$

The next step is to design a control strategy to determine the status of EWHs such that their aggregated power can track this new power reference.

D. LOAD CONTROLLER

A central controller unit should be designed to provide input signals ($m^k(t)$) such that the aggregated power tracks the power reference signal in (22) as accurately as possible.

TABLE 2. EWH parameters.

Model no.	1	2	3	4
Volume, L	150	200	250	300
Rating, kW	1.5	3	3	3
Thermal Capacitance, kWh/°C	0.2	0.25	0.3	0.35
Thermal Resistance, °C/kW	200	138	120	107
Coefficient of performance	1	1	1	1
Temperature set point, °C	58	58	58	58
Temperature dead-band, ($2\delta^k$) °C	4	4	4	4
Number of EWH	125	125	125	125

A time-varying MPC controller is adopted since the first order equation (1) is a linear and time-varying (due to $\theta^k_{in}(t), \theta^k_{out}(t)$ and $\omega^k(t)$ terms). The power error is defined as

$$\varepsilon_p(t) = P_{ref}(t) - P_{agg}(t) \tag{22}$$

thus, the objective function is defined as follows:

$$J_p(t) = \int_t^{t+N_p} \varepsilon_p^2(\tau)\, d\tau \tag{23}$$

Finally, this MPC control function can be found by solving the following optimization problem:

$$\begin{aligned}
&\min J_p(t)\\
&\text{Subject to}\quad \dot{\theta}^k(t) = \frac{1}{R^k C^k}\left(\left(\theta^k_{out}(t) - \theta^k(t)\right)\right.\\
&\left. +\rho c_p R^k \omega^k(t)\left(\theta^k_{in}(t) - \theta^k(t)\right) + R^k m^k(t) P^k_{rate}\right)\\
&m^k(t) = \begin{cases} 1 & \theta^k(t) \le \theta^k_{set} - \delta^k \\ 0 & \theta^k(t) \ge \theta^k_{set} - \delta^k \\ 0 & otherwise\ (OFF\ scenario) \\ 0\ or\ 1 & otherwise\ (ON/OFF\ scenario) \end{cases}\\
&k = 1, \ldots, N
\end{aligned} \tag{24}$$

The optimization problem (24) is not a convex problem and has input signals ($m^k(t)$) with a Boolean constraint. Commercial solvers (i.e., Gurobi) can tackle this type of problem and is subsequently used in this study.

IV. SIMULATION RESULTS AND DISCUSSIONS

A numerical example is simulated to evaluate the effectiveness of the proposed VB-based methodology described in section III. This example considers a homogenous group of four types of EWHs with their individual parameters and manufacturing data being detailed in Table 2 The ambient temperature of the EWH and inlet water temperature are randomized around 20°C and 10°C respectively. The prediction horizon in both the MPC and time varying MPC are assumed to be $N_x = N_p = 3$ minutes.

The nominal behavior of the EWH aggregator assuming internal thermostat control is illustrated in Fig. 3. The figure shows that the simulation starting at midnight lasting for 24 hours and two candidate peak periods are explicit (i.e., local aggregator peaks). The first interval is the morning peak (i.e., 7:00–9:30 am) whereas the second is the evening peak

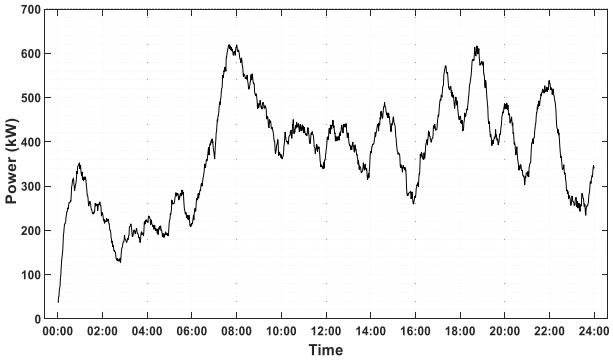

FIGURE 3. Nominal aggregator behavior.

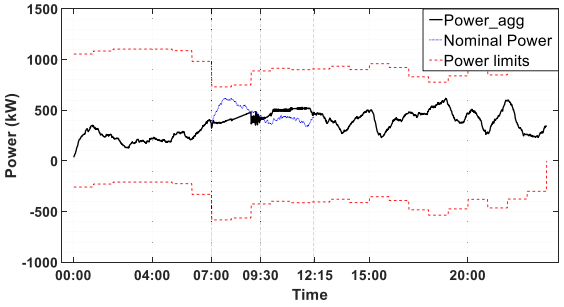

FIGURE 4. Aggregated Power in OFF control scenario.

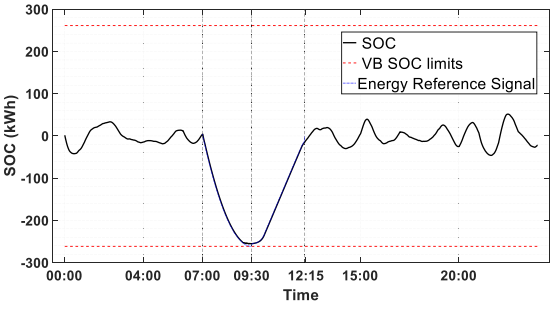

FIGURE 5. VB SOC curve in OFF control scenario.

extends from 17:00 to 20:00 hours. For the sake of simplicity, we assume the optimal benefit scenario where the local and VPP peak period occurred concurrently. This assumption is valid since the EWH aggregator is considered one of the higher power consumption loads [15]. If ON/OFF control is used, a pre-charge period from 5:30 – 7:00 am ensures the VB to be maximally charged prior to the peak shaving period. The reserved aggregator capacity changes according to the EWH control algorithm scenarios (i.e., OFF control or ON/OFF control), see Fig. 5 and Fig. 7. These figures show that the VB has the same upper/lower energy limits in both scenarios, but the energy stored in VB changes dramatically depending on the control algorithm applied. The SOC of the VB in both control scenarios are plotted in Fig. 4 to Fig. 7. Three vertical lines are shown in Fig. 4 and Fig. 5 to distinguish the different control intervals (i.e., peak shaving and payback periods).

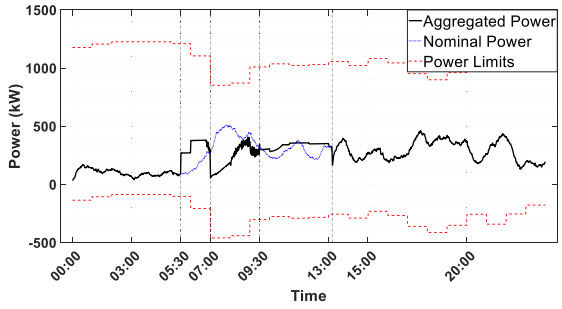

FIGURE 6. Aggregated power in ON/OFF control scenario.

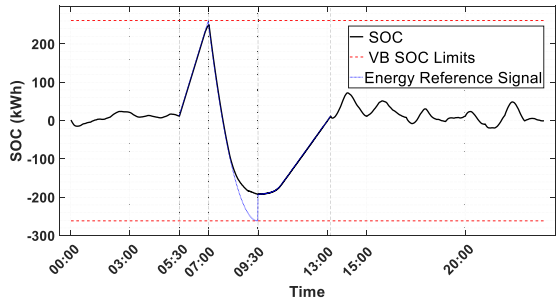

FIGURE 7. SOC curve in ON/OFF control scenario.

Fig. 4 shows the peak shaving process starting at 7:00 am and flattening the desired peak with no dramatic change in the power curve. Fig. 5 illustrates that the SOC of the VB is half charged (i.e., EWHs temperature at the set point level) for the OFF-control scenario. The ON/OFF control scenario results as in Fig. 6 and Fig. 7 shows an additional pre-charging time period prior to the peak shaving and payback time periods. These control periods are separated by four vertical lines in chronological order. The VB capacity and aggregator power limits are made explicit by horizontal dashed lines. The aggregator receives the VPP request at 5:30 AM, i.e., 1:30 hours before the commencement of the peak period. As stated earlier, the pre-charging time period is characterized by the overriding of the thermostat signals with ON signals to facilitate the charging of the VB to its maximum capacity. Smooth charging of the aggregator capacity continues until the VB reaches its maximum capacity at 7:00 AM, as depicted in Fig. 7. The energy reference signal is generated, considering the aggregated power and VB limits as constraints to ensure uniform charging during this time period, as illustrated in Fig. 6 and Fig. 7. This reference signal follows a linear approximation from the current SOC of the VB to its maximum limit. During the interval of 5:30–7:00 AM, Fig. 6 shows that the aggregated power surpasses its nominal level while still respecting the power limits.

The peak shaving process is performed uniformly in the time period between 7:00 AM to 9:30 AM, achieving the requested shaving capacity by forcing the available EWHs to switch OFF. However, reaching the minimum SOC level of the VB depends on the temperature level of each EWH. The VB SOC does not necessarily track the energy reference signal in the case where hot water consumption is minimal and energy losses is mainly through conduction. This is seen at the end of the peak shaving period, see time interval (9:00-9:30 AM in Fig. 5 and Fig. 7. The power curve fluctuations during the same interval in Fig. 4 and Fig. 6, are the result of the controller actions implemented to track the reference line. The controller switches OFF any available EWH to achieve the requested capacity. The VB will be at its lowest capacity if the controller cannot shave sufficient energy.

During the payback time period, the VB is recharged with adequate charging rate reaching to the average SOC. The slope of charging curve determines how much power is required over the baseline without creating a new peak. The VPP control level determines the acceptable level of power to prevent creating a secondary peak when outing together the capacity contributed by all aggregators and system resources. Payback duration is automatically calculated, and the controller generates a reference profile that ensures compliance with the power limits. The payback time is completed around 12:15 PM in the OFF-control scenario as seen in Fig. 4 and Fig. 5, after which the EWHs will revert to internal thermostat. The payback period with ON/OFF control scenario is more complicated, as shown in Fig. 6 and Fig. 7. The ability of this controller to generate ON/OFF signals creates power curves with high fluctuations, especially at the end of peak period. Extra resources and safety precautions (i.e., Short Cycling (SC)) can be used to prevent these fluctuations. SC is defined as the safe time the device holds its old state (ON or OFF) before it can be altered by the controller. It should be noted that SC was not utilized for our research results as the main focus was the inherent controller performance.

Vital performance information gathered for the system operator can be given as follows:

- The VB full storage capacity of the EWHs aggregator is approximately 505 kWh.
- The capacity shaved in both control scenarios are the maximum available as illustrated in Fig. **8**.
- For ON/OFF control scenario:
  - The energy earned during the pre-charge period is 277 kWh with a charging rate of 184.6 kWh/h. The VB is charged at 98% capacity.
  - The average shaved capacity during the peak is 477 kWh which represents 94.7% of the VB capacity with a VB discharge rate of 191 kWh/h.
  - The payback time period registered a 185 kWh above the nominal curve with a duration of 3:30 hours, see Fig. 8.b.
  - The change per device does not reflect a discernible disparity on the daily energy consumption leading to a reduction of less than 0.1kWh.
- For OFF-control scenario:
  - The percentage of peak shaving achieved is 326 kWh representing 64.5% of the VB capacity and 30.2% reduction as compared to ON/OFF scenario, Fig. 8. a.

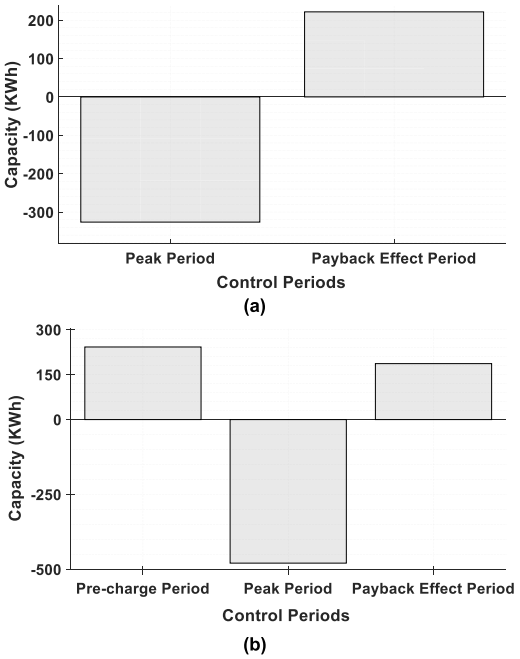

FIGURE 8. Capacity comparison in two control scenarios, (a): OFF control, (b): ON/OFF control.

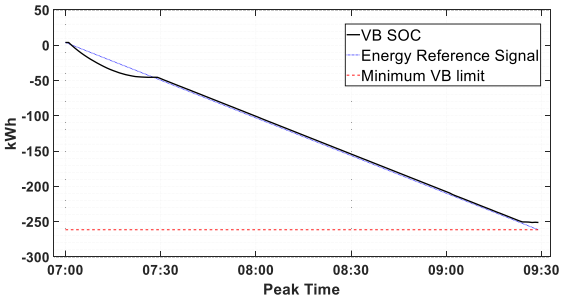

FIGURE 9. Straight line energy reference signal and mismatch period during the peak period.

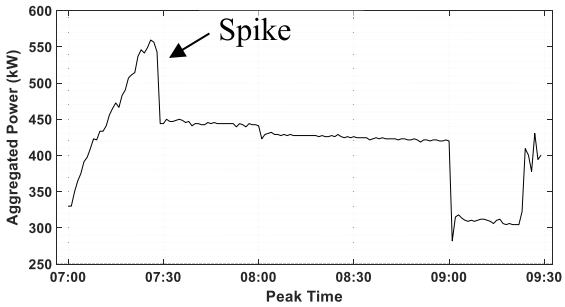

FIGURE 10. Aggregated power and the spike for the valley period.

- The energy gained in the payback period is 222kWh with charging rate of 81.8 kWh/h with duration lasts for 2:45 hours, see Fig. 5.
- The daily energy consumption remains nearly identical, with a recorded reduction per device of 0.39 kWh.

The simulation results for both control scenarios confirm the objective of shifting the power to the Off-peak periods. As expected, the ON/OFF control scenario has greater capacity to share, almost 151 kWh more than energy reserved in the OFF-control scenario. This additional peak shaving capacity is available to the ON/OFF controller due to the utilization of the pre-charging interval. Approximately 55% of the energy gained during the pre-charging is shaved during the peak period. Both algorithms nearly experience the same payback duration, but the energy payback is higher for the ON/OFF control scenario, a penalty for greater peak shaving capacity. The impact of payback can be assessed by introducing the percentage of shaving capacity to the payback duration PP_p as in (25).

$$PP_p = \frac{Shaved\ capacity\ kWh}{samples\ of\ payback\ duration} \tag{25}$$

The PP_p represents the energy compensation at each sample time to safely restore the power balance during the payback period. The value of PP_p for ON/OFF scenario is equal to 2.3 kWh/sample where for OFF control it is 1.34 kWh/sample. These results confirm that the ON/OFF controller has a greater peak shaving capacity given the pre-charging period but results in a higher energy recovery return during the payback period.

A. ENERGY REFERENCE SIGNAL ANALYSIS

The energy reference signal for the peak shaving period is created to utilize the maximum available capacity through the entire peak shaving period. It is only activated during this period as shown in Fig. 9. The energy reference signal guides the VB controller to discharge the energy by broadcasting OFF signals to the TCL devices with a temperature within the hysteresis band. Two forms of this reference signal have been tested to find the maximum energy capacity. Fig. 9 illustrates a straight-line model for the energy reference signal starting from the current SOC till the minimum level SOC of the VB. A mismatch occurs between the energy reference signal and SOC level at the beginning of the peak shaving interval (i.e., Fig. 9, 7:15–07:30 am). It can be explained by 1) the abundant available energy capacity when the VB is charged to the maximum. 2) the number of EWHs that turned OFF by the internal thermostat and 3) the power rating values of EWHs that cannot be fractioned when it turned OFF. This results an undesired power spike illustrated in Fig. 10 within the corresponding time interval in the aggregated power profile. It is apparent that the controller attempts to rectify the mismatch by increasing the power consumption. As a result, the VB SOC should track the energy reference signal as closely as possible during the peak shaving period to limit the impact of this unwanted event.

Reducing any mismatch periods also satisfies the desire to achieve the maximum shaving percentage with minimum impact on customer comfort. Hence, the capacity of the aggregator should be properly distributed over the peak period, especially for long peak durations. This will afford

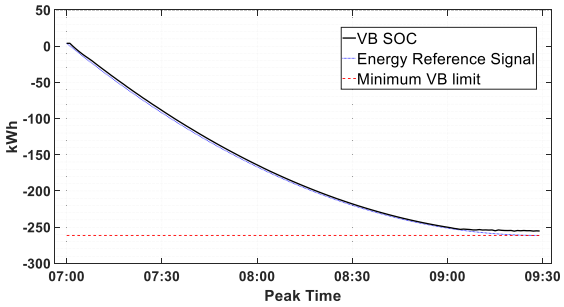

FIGURE 11. Energy reference signal and VB SOC during peak shaving period.

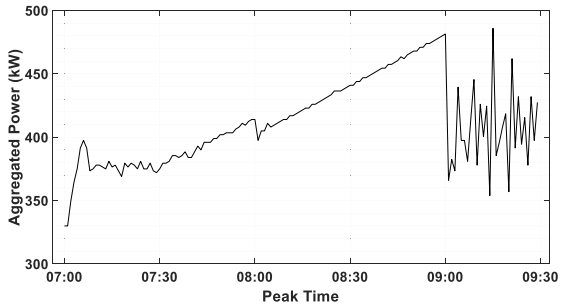

FIGURE 12. Aggregated power during peak shaving.

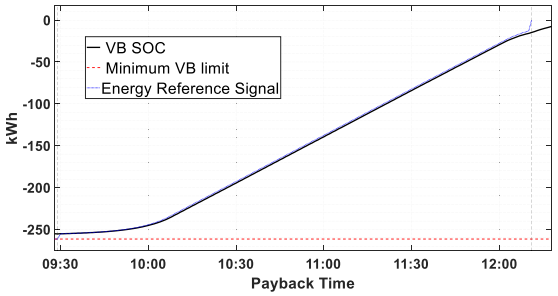

FIGURE 13. Reference signal and VB SOC behavior during payback period.

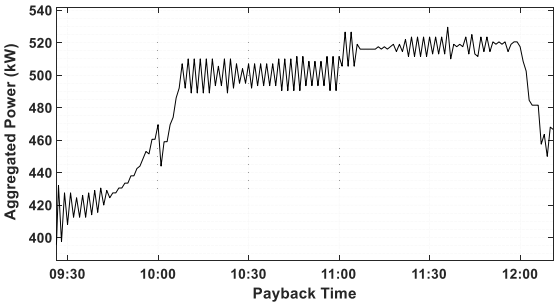

FIGURE 14. Aggregated power during payback period.

sufficient time for other EWHs to become ready to share their capacity. Ultimately, a valid energy reference signal should meet the following conditions: 1) respect the initial SOC of the VB, 2) uniformly distribute the reserve capacity through the whole peak period, and 3) discharge the VB without mismatch periods. Further analysis also shows that peak shaving initially requiring a high VB discharge rate. A low decay curve is then required at the end of the peak period where the reserved capacity is at its minimum. These conditions result in an energy reference signal that follows the parabolic profile shown in Fig. 11. The formulation of this reference signal under the forementioned conditions ensures precise tracking of the maximum reserved energy. In other scenarios, if the capacity of EWHs exceeds the reference requested capacity due to reaching the upper temperature limit, the VB SOC will fail to accurately track the reference, leading to a substantial error $\varepsilon_x(t)$, as shown in Fig. 9. Conversely, if the aggregator lacks sufficient reserved energy, EWHs that are activated due to reaching the lower temperature limit will subsequently turn OFF again. The controller attempts to achieve the requested capacity and subsequently may compromise customer comfort. This scenario can occur with periodic power interruptions in devices with minimal reserved energy. This phenomenon can also prolong the expected payback period, particularly if a significant number of EWHs finished the peak period at the minimum temperature level. Fig. 11 depicts the desired operational behaviour, characterized by minimal deviation between VB SOC and the reference energy signal. The suggested energy reference profile during this period is shown in Fig. 11 where no mismatch in tracking the reference nor spikes are generated in the aggregated power profile as shown in Fig. 12.

The energy reference signal and the controller continue to shift the energy to the payback period. The payback period starts immediately after the peak shaving period by providing a consistent reference profile to charge the VB back to its original nominal value. The controller ensures the optimal shifting of energy, and the control ends before the next peak period starts. The formulation of the energy reference signal during the payback period directly depends on the VB status, capacity available and customer discomfort index. The VPP determines the requirements of the power curve and specifies the consumption limits that must be respected during the payback period. Rapid increases in the VB SOC can result in the creation of a secondary peak in the aggregated power profile and should be avoided. In other words, the goal of the energy reference signal during payback is to ensure a steady increase in the VB SOC without creating a new peak within the VPP constraints. It should also avoid any abrupt changes that may result in response oscillations in the VB SOC or in aggregated power. The duration of the payback period is tied to the power limits set by the VPP and contingent upon the available capacity. Typically, the utility is susceptible to risk, given that a significant portion of energy capacity is utilized during peak periods. We assumed in this study that the power limits during the payback period are within the same range of the power profile during the peak period. The oscillations observed in the payback power profile, as illustrated in Fig. 14 emanate from the controller's attempt to restrain the rapid escalation in the VB charging rate. This measure is taken to avoid any breach of the maximum aggregated power threshold. The payback reference signal and the aggregated power response are shown in Fig. 13 and Fig. 14.

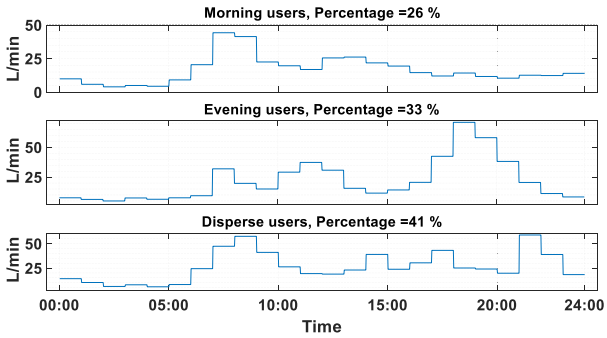

FIGURE 15. The hot water demand profiles scaled to 70,000 habitants.

Fig. 13 illustrates the desired energy reference and the intended tracking of the VB SOC to mitigate any negative impacts. The gradual increase observed initially until 10:00 AM serves multiple objectives, 1) restraining the rapid escalation in the power profile and limit it to an acceptable range, as illustrated in Fig. 14, and 2) establishing a safe margin adjacent to the peak period. The slope of the reference signal ensures a smooth transition back to the internal controller (thermostats) without any abrupt peaks.

B. HOT WATER DEMAND

Hot water demand is the main factor that affects the power demand of EWH aggregators. It is important to accurately model hot water demand profiles since the consumption rate and timing determine the percentage participation of the aggregator [34]. We adopted a hot water demand profile that is based on the consumption probability density function (PDF) reported in [33]. The study divides the day into three consumption periods (i.e., morning, evening, and disperse). The total daily hot water volume is calculated according to the number of occupants in residences and the average day temperature. The daily hot water profile was generated based on the average monthly temperature, number of occupants per house, and demographic statistical data of the city. The aggregated hot water profile for 70,000 users was separated into the three categories mentioned above and are shown in Fig. 15. The results show the average aggregated hot water demand among the three different consumption periods. We randomly selected 500 hot water demand profiles for this research study.

C. SENSITIVITY ANALYSIS

A sensitivity analysis was undertaken to assess the robustness of our proposed peak shaving mechanism. The objective is to examine the variations in the maximum reserved energy capacity in response to changes in other variables. The first study investigated the influence of variations in hot water demand profiles on the maximum reserved energy capacity. Equation (26) shows the effect on water temperature resulting from the increase in hot water demand ($\Delta\omega$), while the corresponding alteration in VB energy is expressed in (27). Four scenarios were examined, each representing a hot water demand increase of 5%, 10%, 15%, and 20%. The results

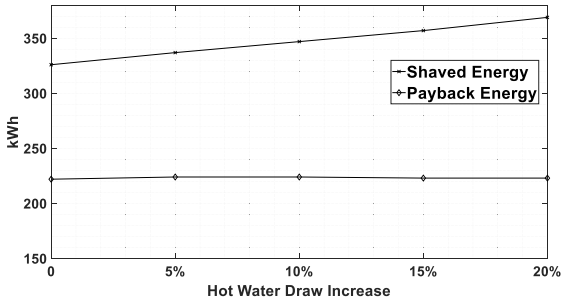

FIGURE 16. Energy capacity change during control periods for OFF control scenario.

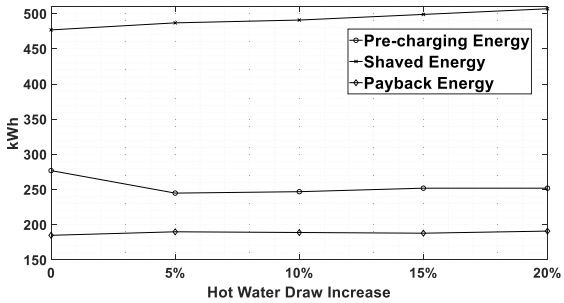

FIGURE 17. Energy capacity change during control periods for ON/OFF control scenario.

obtained from the OFF-control case, as illustrated in Fig. 16, demonstrate that as the hot water demand increases, the amount of shaved energy during peak periods also increases, while the energy gained during payback remains relatively unchanged. These findings suggest that additional peak shaving capacity becomes available with more hot water usage while satisfying power and energy limitations. As expected, Fig. 17 shows that ON/OFF control resulted in more energy savings when compared to the OFF-control scenario. Moreover, the energy required to restore balance during the payback period was less with ON/OFF control compared to the OFF controller. This outcome is primarily attributed to that not all pre-charge energy is consumed in the peak shaving process, allowing for the remaining energy to be invested in the payback period. Both control scenarios exhibit a positive linear correlation between shaved energy and hot water demand. The ON/OFF control scenario demonstrates nearly twice the peak shaving capacity in comparison to the OFF-control scenario. Notably, the trend for payback gained energy remains relatively constant across both control scenarios despite variations in water demand.

$$\dot{\theta}^k(t) + \Delta\dot{\theta}^k = \frac{1}{R^k C^k}\left(R^k P^k(t) + \left(\theta^k_{out}(t) - \theta^k(t)\right) + \rho c_p R^k\left(\omega^k(t) + \Delta\omega^k\right)\left(\theta^k_{in}(t) - \theta^k(t)\right)\right) \quad (26)$$

$$\dot{X}_{agg}(t) + \Delta\dot{X}_{agg} = \alpha(X_{agg}(t) + \Delta X_{agg}) + \beta U(t) \quad (27)$$

Another study investigated the potential change in maximum reserved capacity in the event of communication loss with several EWHs. Two scenarios were considered: firstly, the loss of devices due to power outages, where a linear

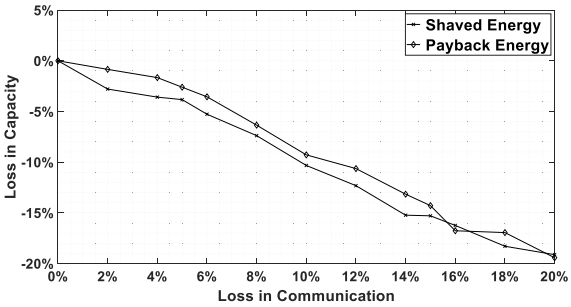

FIGURE 18. Energy capacity change due to communication loss during control period for OFF control scenario.

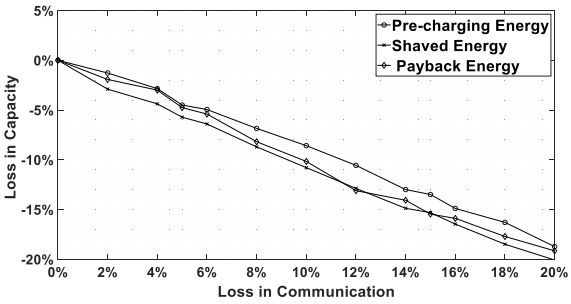

FIGURE 19. Energy capacity change due to communication loss during control periods for ON/OFF control scenario.

relationship was observed, indicating that any lost devices would proportionally reduce the capacity by the same percentage. The second scenario involved only the loss of communication, with affected EWHs being controlled solely by their internal thermostats to meet the constraint outlined in (8). The percentage loss in energy capacity as a function of the percentage loss in communication with EWHs is depicted in Fig. **18** and Fig. **19**. The reference value representing the energy capacity assumes no communication loss (denoted as 0%) with a total of 500 devices. The findings indicate that the aggregator can partially compensate for the loss in devices communication by approximately 2%. The dominance of the linear relation in the sensitivity results can be attributed to factors such as the narrow hysteresis band width (δ^k) of approximately 4° degrees, the algorithm of the external controller, and the normal operation of the TCL device. More noticeable variations in energy capacity would be expected for a broader hysteresis band but this is considered impractical given the design tolerances of the modern EWH. The algorithm of external controller prioritizes EWHs based on their reserved energy during control periods. Therefore, a loss in communication excludes these devices from the controller pool, prompting the selection of alternative devices. Since the goal is to maximize capacity, the outcome is expected to remain relatively consistent. In essence, a loss of 10% of devices results in an approximate 10% reduction in maximum capacity. The maximum recorded discrepancy in this relationship due to communication loss was 2.5%.

V. CONCLUSION

This paper presents an optimized VB-based aggregator as a solution to a challenging problem of estimating the maximum reserved energy of an EWH aggregator required for peak shaving functions. The VB capacity model is based on an aggregation of EWHs with varying sizes and ratings. The study employs a handshaking mechanism that relies on the estimated energy requested and fulfilled between the VPP and the VB. The maximum peak shaving capacities of two EWH control scenarios, OFF and ON/OFF, were compared through simulation. The results indicate that bypassing the EWH's internal thermostat control with ON/OFF control allows for greater peak shaving capacity using the pre-charging stage. The VB model represents a feasible solution for estimating the maximum reserved energy required for peak shaving functions. This is further supported by the model's ability to satisfy internal constraints for both control scenarios, thus indicating its efficacy in regulating energy usage. Additionally, the energy reference signal required by the VB to discharge energy as uniformly as possible is determined. A sensitivity analysis is also conducted to convey the robustness of the proposed TCL aggregation mechanism. The correlation between energy storage capacity and both increased levels of hot water demand and loss in device communications are addressed. Future research will explore alternative peak shaving reference signal shapes to increase the flexibility of energy management and investigating different ancillary service capabilities of the VB aggregator, particularly for services that require more dynamic TCL behavior. Investigating the utilization of the VB as a backup to assign more prosumers energy for P2P trading in the LEM is crucial in future studies. Furthermore, the authors suggest that potential grid stability issues resulting from these demand response initiatives warrant further investigation.

REFERENCES

[1] J. L. Martínez-Godoy, F. Martell-Chávez, I. Y. Sánchez-Chávez, F. A. Castillo-Velásquez, and M. D. C. P. Torres-Falcón, "A peak demand control algorithm for multiple controllable loads in industrial processes," *IEEE Access*, vol. 9, pp. 116315–116325, 2021, doi: 10.1109/ACCESS.2021.3105654.

[2] K. J. Kircher, A. O. Aderibole, L. K. Norford, and S. B. Leeb, "Distributed peak shaving for small aggregations of cyclic loads," *IEEE Trans. Power Del.*, vol. 37, no. 5, pp. 4315–4325, Oct. 2022, doi: 10.1109/TPWRD.2022.3149446.

[3] Q. Zhang and J. Li, "Demand response in electricity markets," in *Proc. 9th Int. Conf. Eur. Energy Mark.*, 2012, pp. 1–8, doi: 10.1109/EEM.2012.6254817.

[4] S. A. Saleh, J. L. Cardenas-Barrera, E. Castillo-Guerra, R. Ahshan, and M. Haj-Ahmed, "An assessment method for smart grid functions in residential loads," in *Proc. 2021 IEEE Ind. Appl. Soc. Annu. Meeting (IAS)*, Oct. 2021, pp. 1–7, doi: 10.1109/ias48185.2021.9677251.

[5] J. Naughton, H. Wang, S. Riaz, M. Cantoni, and P. Mancarella, "Optimization of multi-energy virtual power plants for providing multiple market and local network services," *Electric Power Syst. Res.*, vol. 189, Dec. 2020, Art. no. 106775, doi: 10.1016/j.epsr.2020.106775.

[6] J. Aguilar, C. Bordons, A. Arce, and R. Galán, "Intent profile strategy for virtual power plant participation in simultaneous energy markets with dynamic storage management," *IEEE Access*, vol. 10, pp. 22599–22609, 2022, doi: 10.1109/ACCESS.2022.3155170.

[7] M. Bahloul, L. Breathnach, J. Cotter, M. Daoud, A. Saif, and S. Khadem, "Role of aggregator in coordinating residential virtual power plant in 'StoreNet': A pilot project case study," *IEEE Trans. Sustain. Energy*, vol. 13, no. 4, pp. 2148–2158, Oct. 2022, doi: 10.1109/TSTE.2022.3187217.

[8] H. Hao, B. M. Sanandaji, K. Poolla, and T. L. Vincent, "Aggregate flexibility of thermostatically controlled loads," *IEEE Trans. Power Syst.*, vol. 30, no. 1, pp. 189–198, Jan. 2015, doi: 10.1109/TPWRS.2014.2328865.

[9] F. Ruelens, B. J. Claessens, S. Vandael, B. De Schutter, R. Babuška, and R. Belmans, "Residential demand response of thermostatically controlled loads using batch reinforcement learning," *IEEE Trans. Smart Grid*, vol. 8, no. 5, pp. 2149–2159, Sep. 2017.

[10] S. Xiang, L. Chang, B. Cao, Y. He, and C. Zhang, "A novel domestic electric water heater control method," *IEEE Trans. Smart Grid*, vol. 11, no. 4, pp. 3246–3256, Jul. 2020.

[11] N. Mahdavi and J. H. Braslavsky, "Modelling and control of ensembles of variable-speed air conditioning loads for demand response," *IEEE Trans. Smart Grid*, vol. 11, no. 5, pp. 4249–4260, Sep. 2020, doi: 10.1109/TSG.2020.2991835.

[12] Y. Achour, A. Ouammi, and D. Zejli, "Model predictive control based demand response scheme for peak demand reduction in a smart campus integrated microgrid," *IEEE Access*, vol. 9, pp. 162765–162778, 2021, doi: 10.1109/ACCESS.2021.3132895.

[13] M. Franceschelli, A. Pilloni, and A. Gasparri, "Multi-agent coordination of thermostatically controlled loads by smart power sockets for electric demand side management," *IEEE Trans. Control Syst. Technol.*, vol. 29, no. 2, pp. 731–743, Mar. 2021, doi: 10.1109/TCST.2020.2974181.

[14] H. Gong, V. Rallabandi, M. L. McIntyre, E. Hossain, and D. M. Ionel, "Peak reduction and long term load forecasting for large residential communities including smart homes with energy storage," *IEEE Access*, vol. 9, pp. 19345–19355, 2021, doi: 10.1109/ACCESS.2021.3052994.

[15] Natural Resources Canada. (2017). *Distribution of Residential Energy Use in Canada*. [Online]. Available: https://www.nrcan.gc.ca

[16] M. A. Zu, "Demand response strategy applied to residential electric water heaters using dynamic programming and K-means clustering," *IEEE Trans. Sustain. Energy*, vol. 11, no. 1, pp. 524–533, Jan. 2020.

[17] H. Saele and O. S. Grande, "Demand response from household customers: Experiences from a pilot study in Norway," *IEEE Trans. Smart Grid*, vol. 2, no. 1, pp. 102–109, Mar. 2011, doi: 10.1109/TSG.2010.2104165.

[18] A. Martín-Crespo, S. Saludes-Rodil, and E. Baeyens, "Flexibility management with virtual batteries of thermostatically controlled loads: Real-time control system and potential in Spain," *Energies*, vol. 14, no. 6, p. 1711, Mar. 2021, doi: 10.3390/en14061711.

[19] M. Heleno, M. A. Matos, and J. A. P. Lopes, "Availability and flexibility of loads for the provision of reserve," *IEEE Trans. Smart Grid*, vol. 6, no. 2, pp. 667–674, Mar. 2015, doi: 10.1109/TSG.2014.2368360.

[20] A. Abbas, S. Halbe, and B. Chowdhury, "Comparison of peak demand shaving potential of demand response and distributed energy storage in residential buildings," in *Proc. SoutheastCon*, Apr. 2019, pp. 1–6.

[21] T. Peirelinck, C. Hermans, F. Spiessens, and G. Deconinck, "Domain randomization for demand response of an electric water heater," *IEEE Trans. Smart Grid*, vol. 12, no. 2, pp. 1370–1379, Mar. 2021, doi: 10.1109/TSG.2020.3024656.

[22] V. Lakshmanan, H. Sæle, and M. Z. Degefa, "Electric water heater flexibility potential and activation impact in system operator perspective–Norwegian scenario case study," *Energy*, vol. 236, Dec. 2021, Art. no. 121490, doi: 10.1016/j.energy.2021.121490.

[23] K. Marnell, C. Eustis, and R. B. Bass, "Resource study of large-scale electric water heater aggregation," *IEEE Open Access J. Power Energy*, vol. 7, pp. 82–90, 2020, doi: 10.1109/OAJPE.2020.2967972.

[24] L. A. D. Espinosa, A. Khurram, and M. R. Almassalkhi, "A virtual battery model for packetized energy management," in *Proc. 59th IEEE Conf. Decis. Control (CDC)*, Dec. 2020, pp. 42–48.

[25] L. A. D. Espinosa, A. Khurram, and M. Almassalkhi, "Reference-tracking control policies for packetized coordination of heterogeneous DER populations," *IEEE Trans. Control Syst. Technol.*, vol. 29, no. 6, pp. 2427–2443, Nov. 2021, doi: 10.1109/TCST.2020.3039492.

[26] S. P. Nandanoori, I. Chakraborty, T. Ramachandran, and S. Kundu, "Identification and validation of virtual battery model for heterogeneous devices," in *Proc. IEEE Power Energy Soc. Gen. Meeting (PESGM)*, Aug. 2019, pp. 1–13, doi: 10.1109/pesgm40551.2019.8973978.

[27] S. A. Saleh, J. L. Cardenas-Barrera, E. Castillo-Guerra, B. Alsayid, and L. Chang, "A virtual battery-based method for planning smart grid functions for residential loads," in *Proc. Conf. Rec. Ind. Commer. Power Syst. Tech. Conf.*, Apr. 2021, pp. 1–9, doi: 10.1109/ICPS51807.2021.9416602.

[28] D. Ali, I. Azim, J. Peters, V. Bhandari, A. Menon, and J. Green, "BESS-facilitated local energy market: A case study on typical Australian consumers," in *Proc. 43rd IAEE Int. Conf.*, Aug. 2022, pp. 27–29.

[29] L. Ali, M. I. Azim, J. Peters, V. Bhandari, A. Menon, V. Tiwari, J. Green, and S. M. Muyeen, "Application of a community battery-integrated microgrid in a blockchain-based local energy market accommodating P2P trading," *IEEE Access*, vol. 11, pp. 29635–29649, 2023, doi: 10.1109/ACCESS.2023.3260253.

[30] L. Ali, M. I. Azim, N. B. Ojha, J. Peters, V. Bhandari, A. Menon, J. Green, and S. M. Muyeen, "Integrating forecasting service and Gen2 blockchain into a local energy trading platform to promote sustainability goals," *IEEE Access*, vol. 12, pp. 2941–2964, 2024, doi: 10.1109/ACCESS.2023.3347432.

[31] L. Ali, M. I. Azim, J. Peters, N. B. Ojha, V. Bhandari, A. Menon, V. Tiwari, J. Green, S. M. Muyeen, and M. G. Simoes, "Blockchain-integrated local energy market and P2P trading benefits for participants and stakeholders," in *Proc. IEEE Green Technol. Conf. (GreenTech)*, Apr. 2023, pp. 191–195, doi: 10.1109/GreenTech56823.2023.10173806.

[32] L. Ali, M. I. Azim, J. Peters, E. Pashajavid, V. Bhandari, A. Menon, V. Tiwari, and J. Green, "Local energy markets improve investment returns of residential BESS by arbitrage opportunities," in *Proc. IEEE Sustain. Power Energy Conf. (iSPEC)*, Dec. 2022, pp. 1–5, doi: 10.1109/iSPEC54162.2022.10032992.

[33] D. S. Parker, P. Fairey, and J. D. Lutz, "Estimating daily domestic hot-water use in North American homes," *ASHRAE Trans.*, vol. 121, pp. 258–270, Jun. 2015.

[34] S. Edwards, I. Beausoleil-Morrison, and A. Laperrière, "Representative hot water draw profiles at high temporal resolution for simulating the performance of solar thermal systems," *Sol. Energy*, vol. 111, pp. 43–52, Jan. 2015, doi: 10.1016/j.solener.2014.10.026.

[35] L. Zhao, W. Zhang, H. Hao, and K. Kalsi, "A geometric approach to aggregate flexibility modeling of thermostatically controlled loads," *IEEE Trans. Power Syst.*, vol. 32, no. 6, pp. 4721–4731, Nov. 2017, doi: 10.1109/TPWRS.2017.2674699.

[36] P. Wang, D. Wu, and K. Kalsi, "Flexibility estimation and control of thermostatically controlled loads with lock time for regulation service," *IEEE Trans. Smart Grid*, vol. 11, no. 4, pp. 3221–3230, Jul. 2020, doi: 10.1109/TSG.2020.2973186.

[37] J. T. Hughes, A. D. Domínguez-García, and K. Poolla, "Identification of virtual battery models for flexible loads," *IEEE Trans. Power Syst.*, vol. 31, no. 6, pp. 4660–4669, Nov. 2016, doi: 10.1109/TPWRS.2015.2505645.

[38] P. van Overschee and B. De Moor, *Subspace Identification of Linear Systems: Theory, Implementation, Applications*. New York, NY, USA: Springer, 1996.

ISMAIL ARAFAT (Graduate Student Member, IEEE) received the B.Sc. degree from Cairo University, Egypt, in 2003, and the M.Sc. degree from Al-Balqa' Applied University, Jordan, in 2009. He is currently pursuing the Ph.D. degree with the Emera and NB Power Research Center for Smart Grid Technologies, University of New Brunswick, Fredericton, Canada. His research interests include smart energy systems, demand response, renewable energy, AI applications in power systems, data driven dynamical systems, robotics, and control.

HOSSEIN SHOKOUHINEJAD received the Ph.D. degree in electrical engineering from the University of Tabriz, Iran, in 2017. He is currently a Postdoctoral Fellow with the Department of Electrical and Computer Engineering, University of New Brunswick, Fredericton, NB, Canada. His current research interests include robust control, nonlinear control, robust optimization, and anomaly detection, with application in smart grids, cyber security, switched systems, and gene regulation networks.

EDUARDO CASTILLO GUERRA (Senior Member, IEEE) received the B.Sc. degree in electrical engineering and the M.Sc. degree in telecommunication from the Universidad Central "Marta Abreu" de Las Villas, in 1992 and 1996, respectively, and the Ph.D. degree in electrical engineering from the University of New Brunswick, in 2003. He is currently a Professor with the Department of Electrical and Computer Engineering, University of New Brunswick. His research interests include modeling digital systems, artificial intelligence, smart grids, optimization of renewable energy systems, digital circuit and sensor design, and secure communications. He is a registered Professional Engineer in the Province of New Brunswick, Canada.

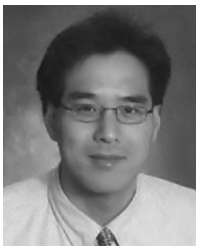

JULIAN MENG (Senior Member, IEEE) received the Ph.D. degree in electrical engineering from Queen's University, Kingston, ON, Canada, in 1993. He is currently the Chair with the Department of Electrical and Computer Engineering, University of New Brunswick, Fredericton, NB, Canada. His research interests include adaptive signal estimation, nonlinear signal processing, renewable energy, and intelligent systems. He is a registered Professional Engineer with APEGNB.

JULIAN L. CARDENAS-BARRERA (Member, IEEE) received the Ph.D. degree in electrical engineering from the Universidad Central "Marta Abreu" de Las Villas, Santa Clara, Cuba, in 1994. Currently, he holds the position of an Associate Professor with the Department of Electrical and Computer Engineering and the NB Power Industrial Research Chair with the Emera and NB Power Research Center for Smart Grid Technologies, University of New Brunswick, Fredericton, NB, Canada. His research focuses on various areas, including the control of renewable energy systems, energy forecasting, communications, and smart grids. He is a registered Professional Engineer in the Province of New Brunswick, Canada.